Journal of Imaging Science and Technology® 53(6): 060504–060504-13, 2009.

Banding Artifact Reduction with Interweaving Dot Dispersion Based on Probability Model and Human Visual System Weighted Root Mean Squared Error in Blue Noise Multilevel Dithering

Tae-Yong Park, In-Su Jang and Yeong-Ho Ha▲
School of Electrical Engineering and Computer Science, Kyungpook National University, 1370 Sankyuk-dong, Buk-gu, Daegu 702-701, Korea
E-mail: yha@ee.knu.ac.kr

Abstract. *Digital printing has focused on multilevel dithering using a stochastic screen as this procedure is simple to implement and yields a smooth output pattern. In bilevel halftoning with a stochastic screen, two printable output levels, i.e., black and white, corresponding to the input image, values are determined by the threshold values of the stochastic screen. For multilevel halftoning, these threshold values are then simply extended using a scaling function. Yet, a simple extension using a scaling function also generates banding artifacts around the intermediate printable tone levels, producing discontinuity in a smooth tone transition region. Therefore, to reduce these banding artifacts, this article proposes blue-noise multilevel dithering with interweaving dot dispersion. First, to investigate the cause and characteristics of the banding artifacts, multilevel halftoning using a simple scaling function is analyzed using a probability model when varying the number of tone levels, thereby generalizing the characteristics of the banding artifacts. The scaling function for the multilevel halftoning is then modified using two control factors based on the generalized characteristics of the banding artifacts according to the number of printable tone levels in order to interweave dot dispersion in the banding regions. The dot distribution across the banding regions is affected by the two control factors that control the interweaving point. The specific values for the control factors are determined by investigating via subjective observation and the human visual system weighted root mean squared error (HVS-WRMSE) curve using the perceived root mean square and based on characteristics of the human visual system. In experiments, an objective evaluation using the HVS-WRMSE of a multitoned image is used to compare the quality of the multitoned patterns around the intermediate tone levels. The proposed method is found to moderately reduce the banding artifacts in the gray ramp when compared to the conventional methods.* © *2009 Society for Imaging Science and Technology.*
[DOI: 10.2352/J.ImagingSci.Technol.2009.53.6.060504]

INTRODUCTION

With the recent advancements in printing technologies, a multilevel ink jet printer is now capable of producing dots with more than two tone levels. This multilevel ink jet printing can be achieved by various approaches, such as using multiple inks with different ink concentrations using variable dot sizes and combinations of these two methods. The halftoning techniques applied to these multilevel systems are generally referred to as multilevel halftoning (multitoning). Multitoning is an extension of bilevel halftoning, which uses black, white, and one or more intermediate tones to produce the appearance of continuous tone images.[1,2]

All bilevel halftoning techniques based on thresholding can be readily generalized and extended to multitoning by replacing the threshold in bilevel halftoning with a multilevel quantizer. Multitoned images exhibit a much lower quantization error than the bilevel case, resulting in a better output quality. Therefore, significant research efforts have been focused on developing appropriate multitoning algorithms for multilevel printing devices.

Faheem et al. suggested a novel multitoning method based on gray-level separation.[3] In this method, the input image is decomposed into printable grayscale images using a set of gray level transformation curves, and each channel is halftoned using a conventional bilevel error diffusion algorithm in a correlated way. Thereafter, the halftoned channels are recombined to obtain the final halftoned image. Although this algorithm is simple to implement and reduces banding artifacts, a high-frequency granularity is maintained in the midtones. In addition, different dot growth patterns are used for low- and high-frequency regions according to the image-dependent characteristics.

Dithering with a stochastic screen for binary halftoning can be easily extended to multitoning using a threshold scaling method. In addition, since the human visual system is less sensitive to blue noise, multitone patterns generated from multilevel dithering with a stochastic screen are less visible to the human observer. Yu et al. proposed an overmodulation method that achieves a smoother transition based on stochastic screening.[4,5] Using this simple technique, the dot patterns around the printable tone levels can be manipulated to introduce the desired multitoned patterns. Yet, even though this algorithm is mean-preserving with respect to the input, special correlations, or special characteristics have to be considered during the screen design as a regular screen is not optimal for this method. Since banding artifacts appear due to a uniform dot distribution around the

▲IS&T Member.

Received Nov. 21, 2008; accepted for publication Jun. 29, 2009; published online Oct. 8, 2009.
1062-3701/2009/53(6)/060504/13/$20.00.

printable tone levels, the dot distribution around these levels must be adjusted by introducing dots of the adjacent tone levels to achieve a smooth tone transition.

Park et al. also proposed banding artifact reduction using an improved threshold scaling function in multitoning with a stochastic screen.[6] The gray level distribution is arranged by controlling the blending proportion of the adjacent output pixels based on threshold scaling functions with two control factors. However, although this method using direct control of the blending proportion has shown improved results compared to previous methods, the control factors determining the blending proportion are obtained through a subjective comparison, inducing instability for the multitoning system.

Yet, all these previous approaches have attempted to reduce the problem of banding artifacts without an in-depth investigation of the banding phenomenon. Thus, the optimized function or parameters need to be reselected with an increase in the printable tone levels and the stochastic screen changed. Accordingly, in this article, the multitoning method with a stochastic screen is generalized into n printable tones, and the reason for and characteristics of the banding artifacts are analyzed when varying the number of printable tones using a probability model. Based on the analytic data, a multilevel dithering method using the interweaving dot-dispersion method is then proposed to reduce the banding artifacts when using regular stochastic screens. The interweaving dot-dispersion method arranges the dot distribution by controlling the proportion of blending dots in the adjacent tone levels.

The proportion of dots in the adjacent tone levels across the banding regions is determined by the two control factors of the dot-dispersion functions that arrange the blending point for the dots in the adjacent tone levels as the sum of the total quantity of the available ink has to be unity, regardless of the image's gray level. To determine a pair of control factors that give a smoother visual transition by blending the dots in the adjacent output levels, the dot distribution around the printable tone levels is subjectively investigated, and then the human visual system weighted root mean squared error (HVS-WRMSE) between the original image and its multitoned version is computed by varying the value of the control factors of the dot-dispersion functions.[7]

In experiments, multitoned images are objectively assessed using the HVS-WRMSE for the gray ramp images. Meanwhile, for a subjective evaluation, several observers compared the results of the proposed method with those of conventional methods by looking at the dot distribution around the printable tone levels.

MULTITONING METHOD USING BLUE NOISE DITHERING

In the bilevel dithering technique based on thresholding with a stochastic screen, an input image value is compared with a corresponding threshold to represent two printable tone levels. This halftoning method can easily be generalized to multitoning due to the simplicity of its implementation, as shown in Figure 1.[4–9] It can be seen that this is equivalent

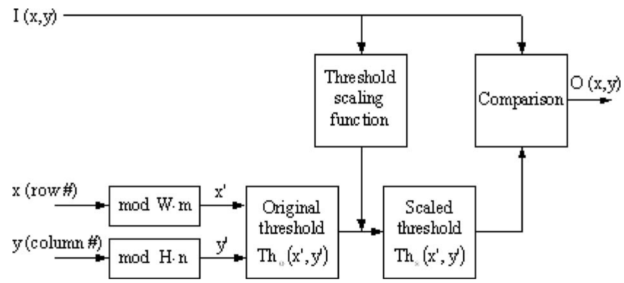

Figure 1. Conventional multitoning scheme with a stochastic screen.

to the binary implementation except that the generalization process requires a threshold scaling step before a comparison is performed as the stochastic screen is currently designed for bilevel halftoning. That is, before an input value is compared pixel by pixel with a corresponding screen threshold, the original threshold range must be scaled to an intermediate range using a threshold scaling function. The output is set to one of the printable tone levels based on the results of the comparison of the input value and the corresponding scaled threshold. For an n-bit input image, the output value of a multilevel ink jet printer with uniform m-tone levels can be expressed as

$$O(x,y) = \frac{2^n - 1}{m-1}k, \quad k = 0,1,\ldots,m-2,m-1. \tag{1}$$

If the input value, $I(x,y)$, is inside the adjacent two tone levels, that is,

$$\frac{2^n - 1}{m-1}(k-1) \le I(x,y) \le \frac{2^n - 1}{m-1}k, \quad k = 0,1,\ldots,m-2,m-1, \tag{2}$$

the original screen threshold, $\mathrm{Th}_o(x',y')$, with n-bit levels from 0 to 2^n-1, is first scaled to a certain intermediate range, as follows:

$$\frac{2^n - 1}{m-1}(k-1) \le \mathrm{Th}_s(x',y') \le \frac{2^n - 1}{m-1}k, \tag{3}$$

where, $\mathrm{Th}_s(x',y')$ is the corresponding scaled threshold. The output value is then set to one of the two tone levels based on the results of the pointwise comparison of the input value and the corresponding scaled threshold:

$$O(x,y) = \begin{cases} \dfrac{2^n - 1}{m-1}k, & I(x,y) \ge \mathrm{Th}_s(x',y') \\ \dfrac{2^n - 1}{m-1}(k-1), & I(x,y) < \mathrm{Th}_s(x',y'). \end{cases} \tag{4}$$

For a color image the original screen threshold must differ for each CMY channel to avoid moiré artifacts, except in the case of dot-on-dot printing. In this case, however, each threshold value can still be scaled by the same process using the threshold scaling function:

$$\mathrm{Th}_s(x',y') = \mathrm{Th}_{s(\max)} + \frac{(\mathrm{Th}_{s(\max)} - \mathrm{Th}_{s(\min)})}{(\mathrm{Th}_{o(\max)} - \mathrm{Th}_{o(\min)})}[\mathrm{Th}_o(x',y') - \mathrm{Th}_{o(\max)}], \quad (5)$$

where Th is an abbreviation of the threshold, and subscripts o and s denote the original and scaled thresholds, respectively. Therefore, $\mathrm{Th}_{o(\max)}$ and $\mathrm{Th}_{o(\min)}$ represent the maximum and minimum values of the original threshold range, which are 2^n-1 and 0, respectively. $\mathrm{Th}_{s(\max)}$ and $\mathrm{Th}_{s(\min)}$ are the large and small values of the intermediate range that will be scaled by Eq. (5), respectively. The relationship between $\mathrm{Th}_{s(\max)}$ and $\mathrm{Th}_{s(\min)}$ is given as

$$\mathrm{Th}_{s(\max)} - \mathrm{Th}_{s(\min)} = \frac{2^n - 1}{m - 1}. \quad (6)$$

Since an intermediate range depends on an input pixel value, Eq. (5) can be explicitly rewritten as follows:

$$\mathrm{Th}_s(x',y') = \frac{2^n - 1}{m - 1}(k-1) + \frac{\mathrm{Th}_o(x',y')}{m-1},$$

$$\frac{2^n - 1}{m - 1}(k-1) \le I(x,y) \le \frac{2^n - 1}{m - 1}k$$

$$k = 1,2,\ldots,m-2,m-1. \quad (7)$$

The relationship between the coordinate system of the image (x,y) and that of the stochastic screen (x',y') is given by the following equation:

$$x = Wm + x',$$

$$y = Hn + y', \quad (8)$$

where W and H denote the width and the height of the stochastic screen, respectively, and m and n are positive integers. The schematic diagram of the threshold scaling for the input value is shown in Figure 2. As such, the output value was set to either $\mathrm{Th}_{s(\max)}$ or $\mathrm{Th}_{s(\min)}$ based on the results of the comparison of the input pixel value and the scaled threshold value at that specific location, which can be expressed as follows:

$$O(x,y) = \begin{cases} \mathrm{Th}_{s(\max)}, & I(x,y) \ge \mathrm{Th}_s(x',y') \\ \mathrm{Th}_{s(\min)}, & I(x,y) < \mathrm{Th}_s(x',y'). \end{cases} \quad (9)$$

The bilevel halftoned version of a 256×128 gray ramp and the multitoned version of the same ramp is illustrated in Figure 3, when a blue noise mask (BNM) was used as the stochastic screen,[10–13] where the general threshold scaling function in Eq. (7) was applied to multitoning. There is a marked similarity between the results of the halftoning and of the multitoning. Each segment of the results of the multitoning could actually be perceived as a scaled version of the results of the halftoning with a compressed tone scale range. This agrees well with the implementation of multitoning as an extension of the bilevel halftoning process.[5] Even though the image that was multitoned using this conventional multitoning scheme exhibited a much smoother tone transition than the bilevel scheme, there was a distinct tone change in the output, which was visible within a certain viewing distance. In other words, when the conventional multitoning scheme was used with the general threshold scaling function, banding artifacts appeared due to

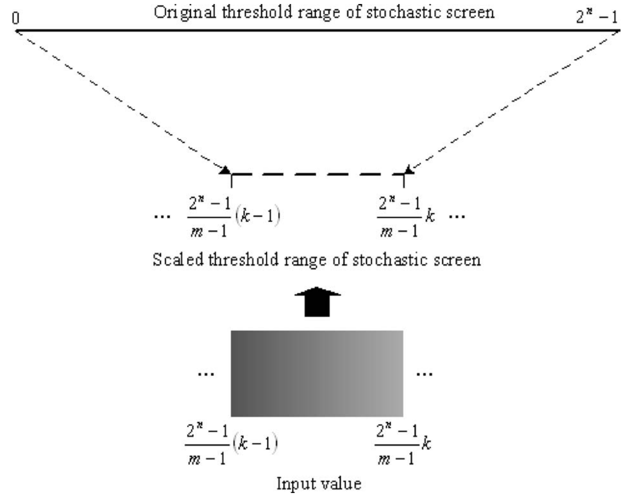

Figure 2. Schematic diagram of threshold scaling, wherein $k=1,2,\ldots,m-2,m-1$.

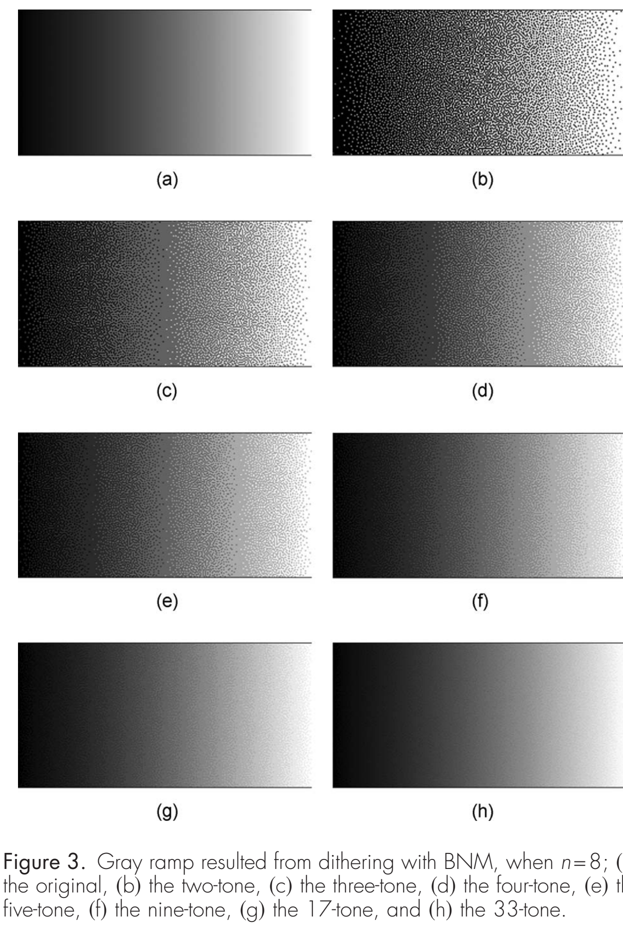

Figure 3. Gray ramp resulted from dithering with BNM, when $n=8$; (a) the original, (b) the two-tone, (c) the three-tone, (d) the four-tone, (e) the five-tone, (f) the nine-tone, (g) the 17-tone, and (h) the 33-tone.

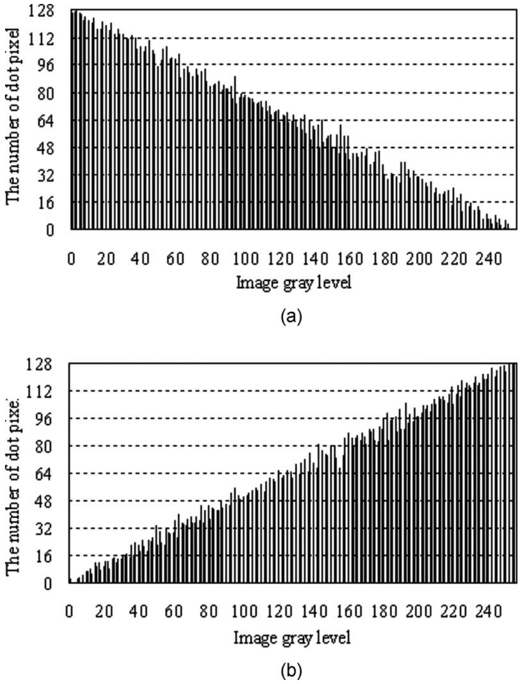

Figure 4. Pixel histogram of the result of the two-tone halftoning in Fig. 3(b); (a) dot pixel of 0 and (b) dot pixel of 255.

the uniform dot distribution around the neighborhoods of the printable tone levels; these resulted in discontinuity and a visually displeasing output pattern in the smooth transition regions.

To investigate the influence of the number of printable tone levels on the width of the perceived banding region, Figures 4 and 5 show a pixel histogram of the results of the bilevel halftoning and the multitoning that correspond to Figs. 3(b) and 3(d). From the histogram graphs, it is evident that slightly removed from the intermediate printable tone levels, there are dot patterns with a sparse distribution of minority dots over a uniform background. As shown in Fig. 3, however, the distribution of the minority dots become denser with the increasing number of printable tone levels, which caused the decrease in the banding width that appears like a band. The symmetrical distribution of the minority dots around the printable tone level of 128 for the uniform three-tone, five-tone, nine-tone, 17-tone, and 33-tone levels and around the printable tone level of 85 for the uniform four-tone level is shown in Figure 6 when an eight-bit input gray ramp was used. It was observed that the increase in the number of printable tone levels resulted in an increasing skewness of the distribution plots for the minority dots around the printable tone levels of 128 and 85, which affected the width of the perceived banding region.

ANALYSIS FOR BANDING ARTIFACT BASED ON PROBABILITY MODEL

This banding artifact around the intermediate printable tone level can be explained using the probability model.[14] In the case of the bilevel halftoning, let the eight-bit input image in the halftoning process be $I[x,y]$, a continuous-tone discrete-space monochromatic image with gray values between 0 (black) and 255 (white). The output is a binary discrete-space image, $O[x,y]$. Of particular interest are the binary patterns, $O[x,y;g]$, that resulted from the dithering of an input patch image of only one fixed gray value, $I[x,y]=g$. The aperiodic patterns can be modeled as stochastic processes. The unconditional probability mass function of any individual binary output pixel, $O[x,y;g]$, is

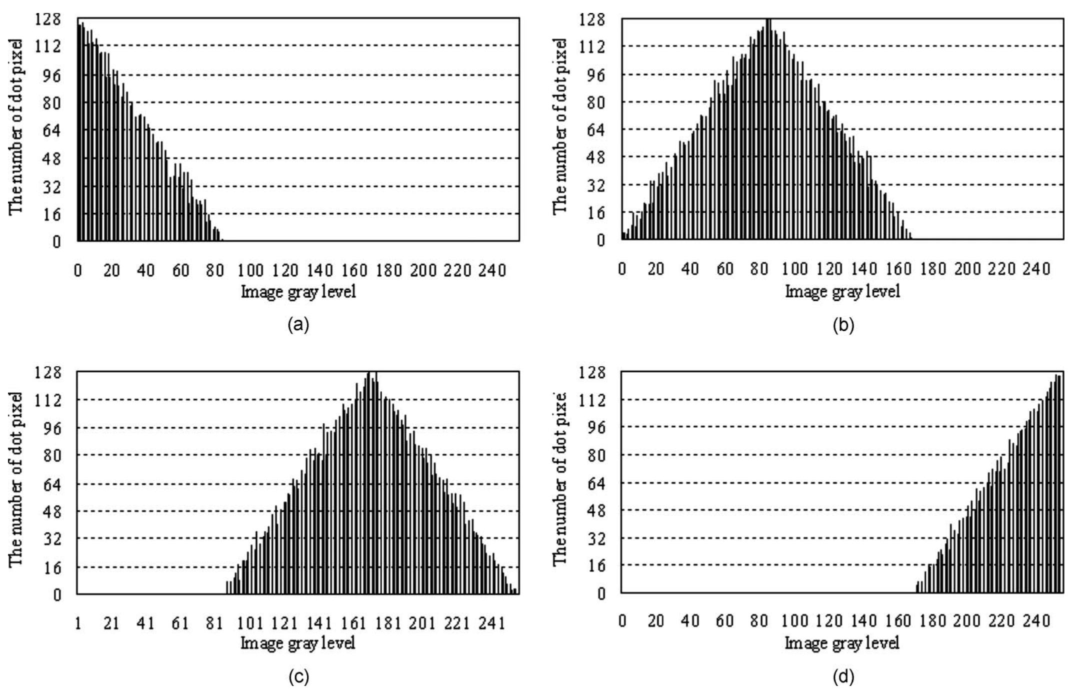

Figure 5. Pixel histograms of the result of the four-tone multitoning in Fig. 3(d); (a) dot pixel of 0, (b) dot pixel of 85, (c) dot pixel of 170, and (d) dot pixel of 255.

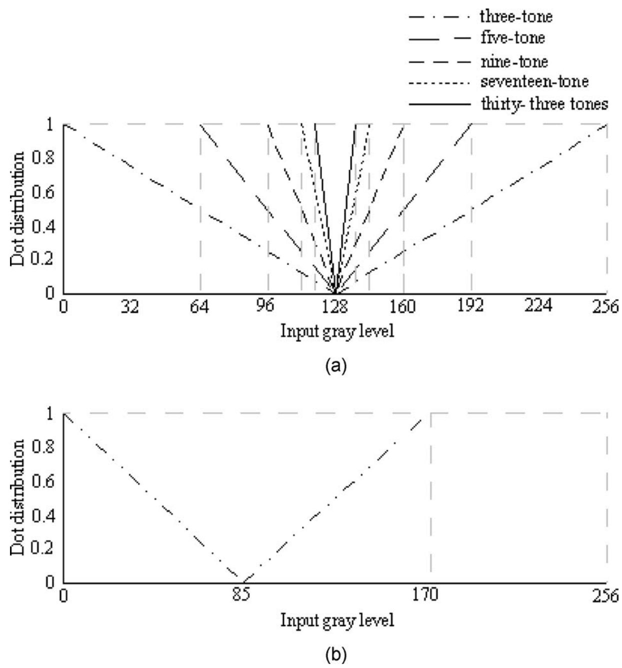

Figure 6. Distribution plots of the minority dots around the intermediate printable tone level; (a) for the uniform three-tone, five-tone, nine-tone, 17-tone, and 33 tone images and (b) for the uniform four-tone image.

$$P_o(O[x,y;g]) = \begin{cases} \dfrac{g}{255}, & \text{for} \quad O[x,y;g] = 255 \\ 1 - \dfrac{g}{255}, & \text{for} \quad O[x,y;g] = 0. \end{cases} \tag{10}$$

This probability mass function in terms of the gray level g is shown in Figure 7(a), which is a discrete distribution with two possible outcomes. It can thus be modeled as a Bernoulli distribution. Since this is true for all $[x,y]$, $O[x,y;g]$ is a stationary random process with

$$E\{O[x,y;g]\} = g \tag{11}$$

and

$$\mathrm{var}\{O[x,y;g]\} \equiv \sigma_g^2 = \frac{g}{255}\left(1 - \frac{g}{255}\right). \tag{12}$$

The mean of $O[x,y;g]$ is exactly what is expected since it represents the gray level g. The variance of $O[x,y;g]$ varies with g and peaks at $g=255/2$, midway between the extremes of zero variance at the solid black and white, as shown in Fig. 7(a).

In the case of the multitoning with the n-bit input image and the uniform m-tone printable levels, the unconditional probability mass function for $(2^n-1)/(m-1)(k-1) \leq g \leq (2^n-1)/(m-1)k$ and $(2^n-1)/(m-1)k \leq g \leq (2^n-1)/(m-1)(k+1)$, where $k=1,2,\ldots,m-3,m-2$, is given as follows:

$$P_0(O[x,y;g]) = \begin{cases} \dfrac{m-1}{2^n-1}g-(k-1), & \text{for} \quad O[x,y;g] = \dfrac{2^n-1}{m-1}k \\ k-\dfrac{m-1}{2^n-1}g, & \text{for} \quad O[x,y;g] = \dfrac{2^n-1}{m-1}(k-1), \end{cases}$$

$$\frac{2^n-1}{m-1}(k-1) \leq g \leq \frac{2^n-1}{m-1}k, \tag{13}$$

and

$$P_0(O[x,y;g]) = \begin{cases} \dfrac{m-1}{2^n-1}g-k, & \text{for} \quad O[x,y;g] = \dfrac{2^n-1}{m-1}(k+1) \\ (k+1)-\dfrac{m-1}{2^n-1}g, & \text{for} \quad O[x,y;g] = \dfrac{2^n-1}{m-1}k, \end{cases}$$

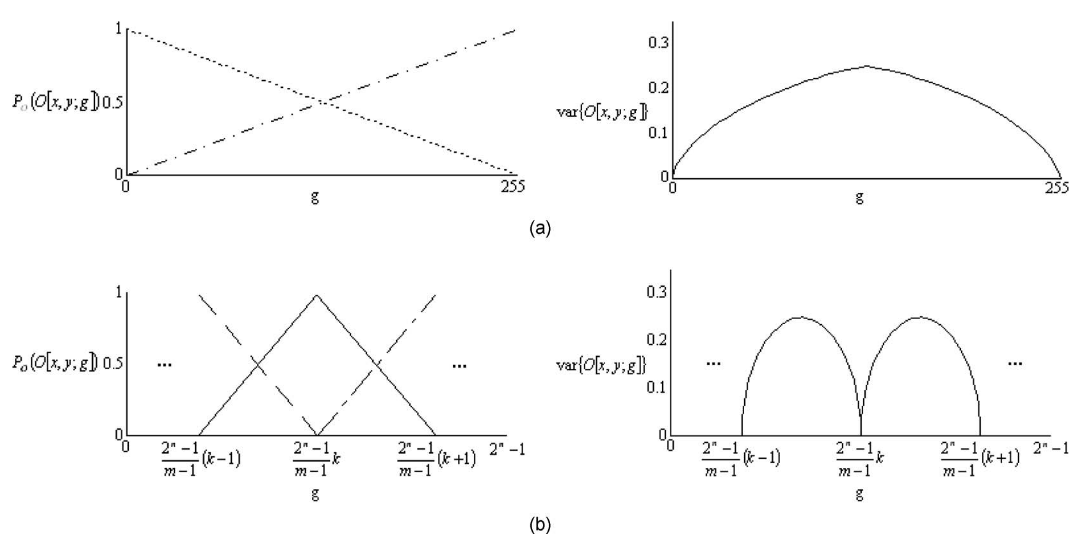

Figure 7. Probability mass function and Variance of $O[x,y;g]$ vs the gray level g; (a) in bilevel halftoning and (b) in multitoning.

$$\frac{2^n-1}{m-1}k \le g \le \frac{2^n-1}{m-1}(k+1). \tag{14}$$

These functions in terms of the gray level g are shown in Fig. 7(a). At the intermediate printable tone levels, there is no distribution of the minority dots because the ink for that particular level is available. Slightly away from these levels, the probability distribution of the minority dots, which looks like a band, gradually increases.

The mean of $O[x,y;g]$ for both cases is g and the variance of $O[x,y;g]$ is

$$\mathrm{var}(O[x,y;g]) = \left(\frac{m-1}{2^n-1}g-(k-1)\right)\left(k-\frac{m-1}{2^n-1}g\right) = -\left(\frac{m-1}{2^n-1}g-\frac{2k-1}{2}\right)^2+\left(\frac{2k-1}{2}\right)^2 - k(k-1),$$

$$\frac{2^n-1}{m-1}(k-1) \le g \le \frac{2^n-1}{m-1}k, \tag{15}$$

and

$$\mathrm{var}(O[x,y;g]) = \left(\frac{m-1}{2^n-1}g-k\right)\left((k+1)-\frac{m-1}{2^n-1}g\right) = -\left(\frac{m-1}{2^n-1}g-\frac{2k+1}{2}\right)^2+\left(\frac{2k+1}{2}\right)^2 - k(k+1),$$

$$\frac{2^n-1}{m-1}k \le g \le \frac{2^n-1}{m-1}(k+1). \tag{16}$$

For the multitoning, the mean of $O[x,y;g]$ is exactly what was expected. The variance of $O[x,y;g]$ varied with g and k had a maximum at the middle of the two adjacent printable tone levels and had a minimum at the printable tone levels, as shown in Fig. 7(b). The distribution of the dots of the printable tone levels in the multitoning is illustrated in Figure 8 when a general threshold scaling function was used. In Fig. 8, the dots of the printable tone levels are symmetrically distributed around the intermediate tone levels, and dots of the adjacent printable tone levels are not introduced at these points owing to the low variance of the binary pattern, resulting in banding artifacts.

PROPOSED MULTILEVEL DITHERING USING INTERWEAVING DOT-DISPERSION METHOD

To achieve a smoother visual transition while preserving the mean level of the input image, the dot distribution must to be adjusted by introducing dots of the adjacent tone levels in the region where the banding artifacts are dominant. Since banding artifacts may appear due to a uniform dot distribution caused by low variance of the binary pattern, the dot

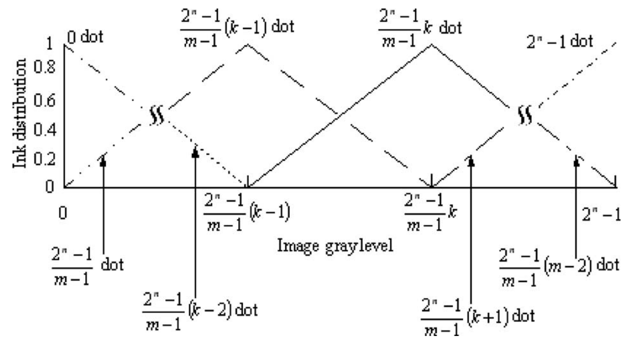

Figure 8. Distribution of the dots of the printable tone levels in multitoning using a general threshold scaling function, wherein $k=2,3,\ldots,m-3$, $m-2$.

patterns around the intermediate tone levels must be manipulated to achieve the desired multitone patterns. To accomplish this, the distribution plot of the dots must be flattened and crossed in the banding regions by introducing dots of the adjacent tone levels.

In the case of conventional multilevel dithering, when a general threshold scaling function is used, as shown in Fig. 8, the only printable tone level available is $(2^n-1)k/(m-1)$, where $k=0,1,\ldots,m-2,m-1$ in each region where banding artifacts are dominant. However, in Figure 9(a), the linear combination of dots from adjacent tone levels around the intermediate tone levels can reduce unwanted banding artifacts in a multitoned image. For example, to reproduce a $(2^n-1)k/(m-1)$ image gray level, $(2^n-1)(k-2)/(m-1)$ dots, $(2^n-1)(k-1)/(m-1)$ dots, and $(2^n-1)k/(m-1)$ dots are utilized by adjusting the distribution of dots for the printable tone levels between $B1_-$ and $B1_+$. As shown in Fig. 9(b), the control factors, $B1_-$ and $B1_+$,

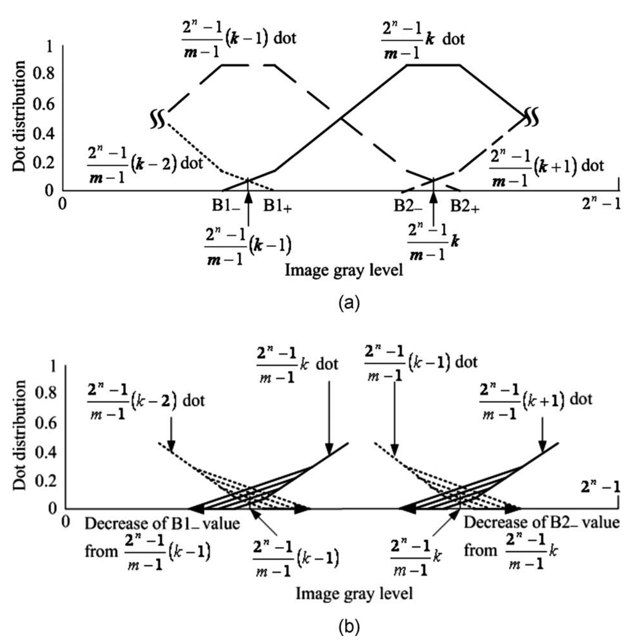

Figure 9. (a) Desired distribution plot of the dots for the multitoned gray ramp and (b) control of the blending proportion of the dots of the adjacent tone levels wherein $k=2,3,\ldots,m-3,m-2$.

determine the blending proportion of dots from the adjacent tone levels. However, since a discontinuous change in the reproduced tone can be induced by the blending proportion, the control factors should be determined based on considering a smooth visual transition. Consequently, the control factors are estimated using the perceived root mean squared error between the original image and its multitoned version and then compared with the results of a subjective evaluation.

QUANTIZATION TO DETERMINE THE PROPORTION OF THE MAJORITY DOTS

With an input value at a specific location, the first step checks whether it is inside the neighborhood of any intermediate printable tone levels. If not, the conventional multitoning method using a general threshold scaling function is applied, wherein quantization by pointwise comparison of the input value and the scaled threshold value is carried out to simply determine the output value. Otherwise, when an input pixel is within the neighborhood of any printable tone level, quantization is first performed in order to determine the proportion of the majority dots inside the banding regions.

As used herein, the term "majority dot" in a binary halftone pattern refers to a dot that corresponds to a dot distribution larger than 0.5. The term "minority dot" refers to a dot that corresponds to a dot distribution smaller than 0.5.[15] More specifically, consider a binary image pattern consisting of dots with one of two states, which can be thought of as *black* and *white*. In any given binary pattern, there will always be more dots of one state, the majority dots, than in the other, the minority dots, except for the special case where there is exactly the same number of each state. Similar to the halftoning case, the majority dots, p_m, for each banding region are defined as follows:

$$p_m = \begin{cases} \dfrac{2^n-1}{m-1}(k-1), & I(x,y) = [B1_-, B1_+] \\ \dfrac{2^n-1}{m-1}k, & I(x,y) = [B1_-, B1_+], \end{cases} \tag{17}$$

and the minority dots, P_a, which are equal to the dots of the adjacent tone levels, are

$$p_a = \begin{cases} \dfrac{2^n-1}{m-1}(k-2) \text{ and } \dfrac{2^n-1}{m-1}k, & I(x,y) = [B1_-, B1_+] \\ \dfrac{2^n-1}{m-1}(k-1) \text{ and } \dfrac{2^n-1}{m-1}(k+1), & I(x,y) = [B2_-, B2_+], \end{cases} \tag{18}$$

where $B1_-$ and $B2_-$ represent the gray levels of the starting point, and $B1_+$ and $B2_+$ correspond to the gray levels of the finishing point for each banding region, as shown in Fig. 9(a).

The quantization process is expressed as a pointwise comparison between the fixed input value and the corresponding threshold value scaled by a general threshold scaling function. The output value is determined as one of the majority dots and the dots of the adjacent tone levels according to the quantization results with respect to the extent of the given input value. The introduction of the dots of the adjacent tone levels allows the peak of the distribution plot of the majority dots to be flattened in the neighborhood of the printable tone levels of $(2^n-1)(k-1)/(m-1)$ and $(2^n-1)k/(m-1)$, as shown in Fig. 9(a). The quantization can be expressed as

$$O(x,y) = \begin{cases} p_m, & I_f(x,y) \geq \mathrm{Th}_s(x',y') \\ p_a, & I_f(x,y) < \mathrm{Th}_s(x',y'), \end{cases}$$

$$\text{for } I(x,y) = \left[B1_-, \frac{2^n-1}{m-1}(k-1)\right] \text{or} \left[B2_-, \frac{2^n-1}{m-1}k\right], \tag{19}$$

and

$$O(x,y) = \begin{cases} p_m, & I_f(x,y) \leq \mathrm{Th}_s(x',y') \\ p_a, & I_f(x,y) > \mathrm{Th}_s(x',y'), \end{cases}$$

$$\text{for } I(x,y) = \left[\frac{2^n-1}{m-1}(k-1), B1_+\right] \text{or} \left[\frac{2^n-1}{m-1}k, B2_+\right], \tag{20}$$

where $O(x,y)$ is the output value and $I_f(x,y)$ represents the fixed input value that corresponds to the increasing input value in the banding regions, which are shown in Figure 10. Using the fixed input value instead of the increasing input gray level, we find that the proportion of the majority dots is controlled. Since there is a constraint condition that the sum of the total quantity of the available ink has to be one regardless of the image gray level, however, the fixed input values had to be determined by taking into account the proportions of the dots of the adjacent tone levels. The distribution of the dots of the adjacent tone levels in a given proportion were determined using the dot-dispersion functions, which will be presented in the following section.

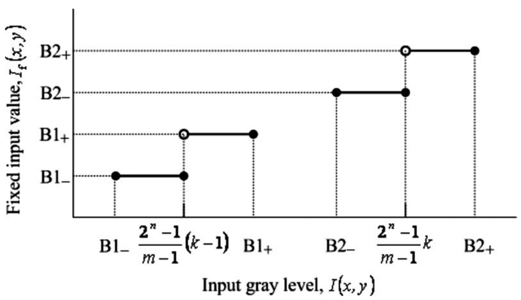

Figure 10. Fixed input values that correspond to the increasing input value.

QUANTIZATION TO BLEND DOTS OF ADJACENT TONE LEVELS

To preserve the gray-level balance near the printable tone levels, the dot distribution had to be adjusted by blending the majority dots with the dots of the adjacent tone levels. As indicated in Eqs. (19) and (20), if the output of the quantization in the previous section is not a majority dot, the dots of the adjacent tone levels had to be printed. For each banding region, two sorts of dots of the adjacent tone levels were available, as given in Eq. (18). Therefore, the dot proportion determined by the blending point for the dots of the adjacent tone levels had to be carefully determined to achieve a visually smooth tone transition in each banding region. This article thus proposes a blue noise multilevel dithering technique using the dot-dispersion method so that the dot distribution could be arranged by controlling the blending proportion of the dots of the adjacent tone levels. The proposed dot-dispersion functions have two control factors that handle the blending point of the dots of the adjacent tone levels in each banding region. The dot-dispersion functions, represented as the gray level that corresponds to the starting point of each banding region, are given as follows:

$$\mathrm{Th}_s(x',y') = \frac{2^n-1}{m-1}(k-2) + \frac{\mathrm{Th}_o(x',y')}{m-1}$$

$$\mathrm{Th}_{ss}(x',y') = B1_- + [\mathrm{Th}_s(x',y') - B1_-]2,$$

$$\text{for} \quad I(x,y) = \left[B1_-, \frac{2^n-1}{m-1}(k-1) \right], \tag{21}$$

$$\mathrm{Th}_s(x',y') = \frac{2^n-1}{m-1}(k-1) + \frac{\mathrm{Th}_o(x',y')}{m-1},$$

$$\mathrm{Th}_{ss}(x',y') = B1_- + \left[\mathrm{Th}_s(x',y') - \frac{2^n-1}{m-1}(k-1) \right]2,$$

$$\text{for} \quad I(x,y) = \left[\frac{2^n-1}{m-1}(k-1), B1_+ \right], \tag{22}$$

$$\mathrm{Th}_s(x',y') = \frac{2^n-1}{m-1}(k-1) + \frac{\mathrm{Th}_o(x',y')}{m-1},$$

$$\mathrm{Th}_{ss}(x',y') = B2_- + [\mathrm{Th}_s(x',y') - B2_-]2,$$

$$\text{for} \quad I(x,y) = \left[B2_-, \frac{2^n-1}{m-1}k \right], \tag{23}$$

and

$$\mathrm{Th}_s(x',y') = \frac{2^n-1}{m-1}(k-1) + \frac{\mathrm{Th}_o(x',y')}{m-1},$$

$$\mathrm{Th}_{ss}(x',y') = B2_- + \left[\mathrm{Th}_s(x',y') - \frac{2^n-1}{m-1}k \right]2,$$

$$\text{for} \quad I(x,y) = \left[\frac{2^n-1}{m-1}k, B2_+ \right], \tag{24}$$

where $\mathrm{Th}_{ss}(x',y')$ denotes the twice-scaled threshold for the original threshold, $\mathrm{Th}_o(x',y')$, and $B1_-$ and $B2_-$ are the two control factors that represent the gray levels corresponding to the blending point of the dots from the adjacent tone levels in each banding region, as shown in Fig. 10. In this step, the final output is determined as one of the dots of the adjacent tone levels, depending on the pointwise comparison of the input value and the corresponding twice-scaled threshold value. The quantization processes are given as

$$O(x,y) = \begin{cases} \frac{2^n-1}{m-1}k, & I(x,y) \geq \mathrm{Th}_{ss}(x',y') \\ \frac{2^n-1}{m-1}(k-2), & I(x,y) < \mathrm{Th}_{ss}(x',y'), \end{cases}$$

$$\text{for} \quad I(x,y) = [B1_-, B1_+], \tag{25}$$

and

$$O(x,y) = \begin{cases} \frac{2^n-1}{m-1}(k+1), & I(x,y) \geq \mathrm{Th}_{ss}(x',y') \\ \frac{2^n-1}{m-1}(k-1), & I(x,y) < \mathrm{Th}_{ss}(x',y'), \end{cases}$$

$$\text{for} \quad I(x,y) = [B2_-, B2_+]. \tag{26}$$

To explain the principle behind the dot-dispersion functions, the process of threshold scaling for the region from $(2^n-1)(k-2)/(m-1)$ to $(2^n-1)(k-1)/(m-1)$ is shown in Figure 11. The decrease in the value from $(2^n-1)(k-1)/(m-1)$ controlled not only the premature introduction but also the final determination of the dots of the adjacent tone levels in the quantization process due to the increase in the twice-scaled threshold.

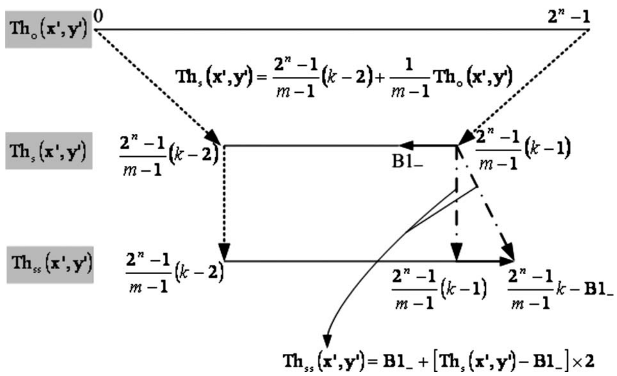

Figure 11. Dot-dispersion function process for the region from $(2^n-1)\times(k-2)/(m-1)$ to $(2^n-1)(k-1)/(m-1)$.

To determine the pair of control factors, $(B1_{-}, B2_{-})$ that would give a better tone representation and better overall quality as well as to eliminate the undesirable banding artifacts near the printable tone levels, gray patches for each level were generated and multitoned using the proposed method with the specific value of the control factors, and the HVS-WRMSE was calculated for each patch. Moreover, the HVS model of Sullivan et al.[7] was utilized to study the perceived root mean square error between the original image and its multitoned version. If $h[m,n]$ is the point spread function of a human eye, the error is given by

$$e = \sqrt{\frac{\Sigma\Sigma(x[m,n]*h[m,n]-y[m,n]*h[m,n])^2}{N}}, \tag{27}$$

where "$*$" stands for the circular convolution and N is the number of total pixels. In the spatial frequency domain, the equation is as follows:

$$E = \sqrt{\frac{\Sigma\Sigma(X[i,j]-Y[i,j])\times H[i,j]}{N}}. \tag{28}$$

A model of the low-contrast photopic modulation transfer function (MTF) below was used to characterize the HVS (Ref. 7):

$$H[i,j] = \begin{cases} a(b+cf_{ij})\exp[-(cf_{ij})^2] & f_{ij} > f_{\max} \\ 1.0, & f_{ij} \le f_{\max}, \end{cases} \tag{29}$$

where the constants a, b, c, and d take on the values 2.2, 0.192, 0.114, and 1.1, respectively. To apply this model to a specific viewing distance and resolution, a conversion from cycles/degree to cycles/in. was also carried out. A plot of the visual model for a 10 in. viewing distance and 400 dots/in. is shown in Figure 12, which illustrates the low-pass nature of the visual system.

The results of the multitoning using the conventional multitoning method with a general threshold scaling function and the corresponding HVS-WRMSE curve are shown in Figure 13(a). In a similar manner, Figs. 13(b)–13(d) show the gray ramp images that were multitoned using the proposed method, with the specific value of the two control factors and the corresponding HVS-WRMSE curves. As shown in Fig. 13(a), around each intermediate tone level (85 and 170 in this case), there is a distinct dipping and shoot up of the HVS-WRMSE. Slightly away from those levels, the human eye tends to pick up those dots very easily due to the dot patterns with a sparse distribution of the minority dots over a uniform background, which results in high visual errors. The distribution plots of the dots that correspond to Fig. 13 are also shown in Figure 14. Clearly, decreasing the $B1_{-}$ and $B2_{-}$ values from the tone levels results in the introduction of the dots of the adjacent tone levels in the distribution and flattening of the skewness of the distribution plots of the dots across the banding region. As a result, the desired distribution plot for the dots of the adjacent tone levels was achieved around the printable tone levels. Also, as the dots of the adjacent tone levels in the distribution were introduced around the intermediate printable tone levels, the visual errors in these regions were more considerably reduced. Consequently, the significant reduction in the HVS-WRMSE was also resolved. The premature introduction of the dots of the adjacent tone levels in the distribution increased, however, the graininess of the image, resulting in the fluctuation of the HVS-WRMSE, as shown in Fig. 13. For the dot distributions, wherein the introduction of the minority dots was sufficient to get rid of the banding artifacts and when the two control factors of $B1_{-}$ and $B2_{-}$ were 81 and 166, respectively, it was observed that the HVS-WRMSE value at the intermediate printable tone levels was almost equal to the neighboring value. Therefore, the banding artifact was sufficiently removed, and the gray-level balance was adequately maintained with this specific control factor.

To closely observe the change in the HVS-WRMSE when the two control factors around the printable tone levels were varied, the extent of the significant dipping in the HVS-WRMSE was investigated, as shown in Figure 15. Here, the width, W, is defined as the gray-level difference in the two crossing points between the HVS-WRMSE curve and its average line. Also, the difference between the average value and the minimum value in the HVS-WRMSE is defined as the depth, D. The subscripts stand for the intermediate printable tone levels when uniform four-tone levels were used. From Table I, as the control factors moved slightly away from the intermediate printable tone levels, the width and depth of

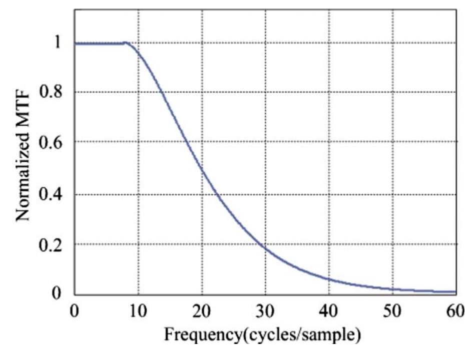

Figure 12. HVS model used for the evaluation.

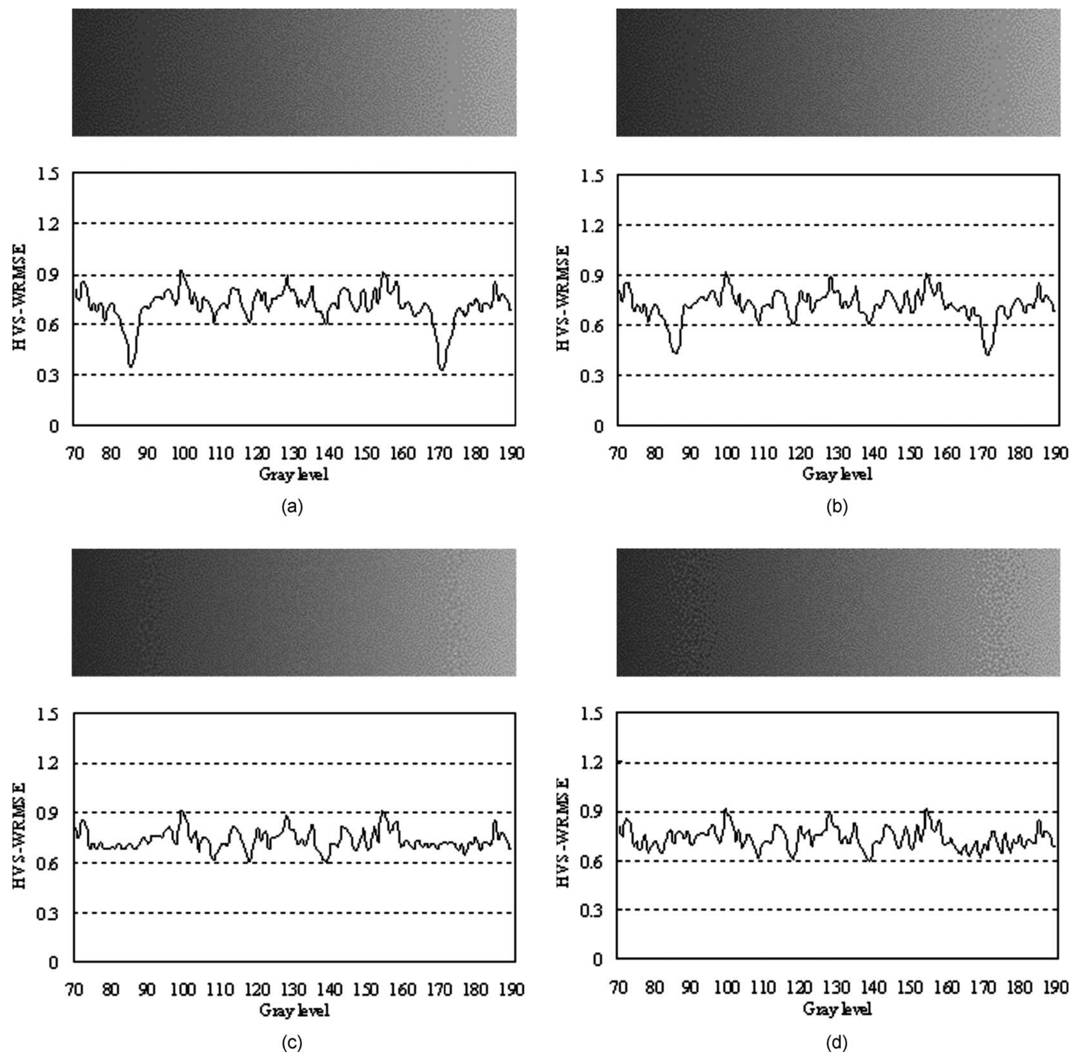

Figure 13. Multitoned gray ramp image and its HVS-WRMSE using (a) the general threshold scaling function, (b) two control factors with $(B1_{-}, B2_{-})=(84, 169)$, (c) two control factors with $(B1_{-}, B2_{-})=(81, 166)$, and (d) two control factors with $(B1_{-}, B2_{-})=(78, 163)$.

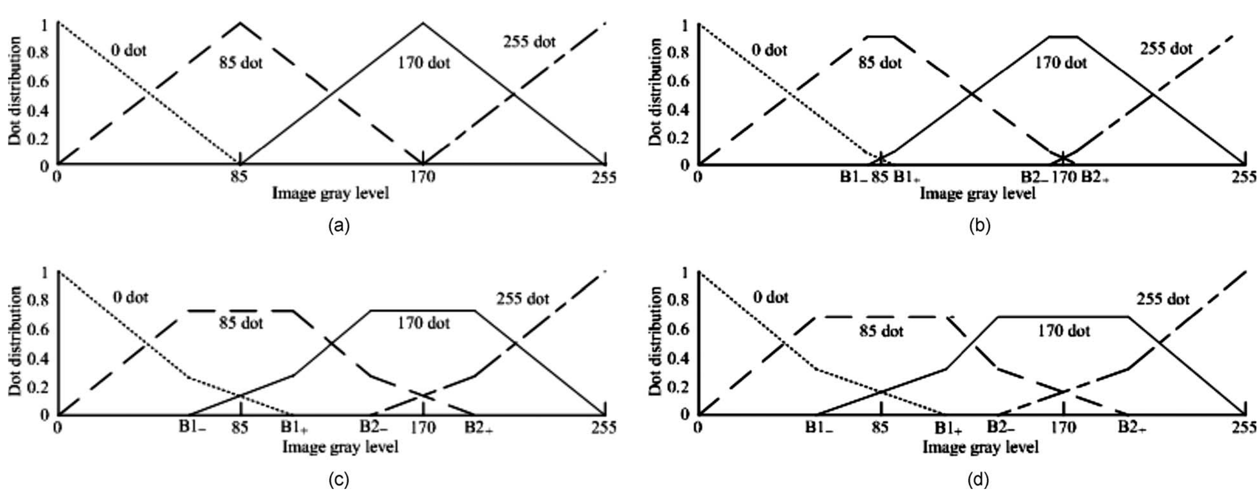

Figure 14. Dot distribution of the multitoned gray ramp; using (a) a general threshold scaling function, (b) two control factors with $(B1_{-}, B2_{-})=(84, 169)$, (c) two control factors with $(B1_{-}, B2_{-})=(81, 166)$, (d) two control factors with $(B1_{-}, B2_{-})=(78, 163)$,

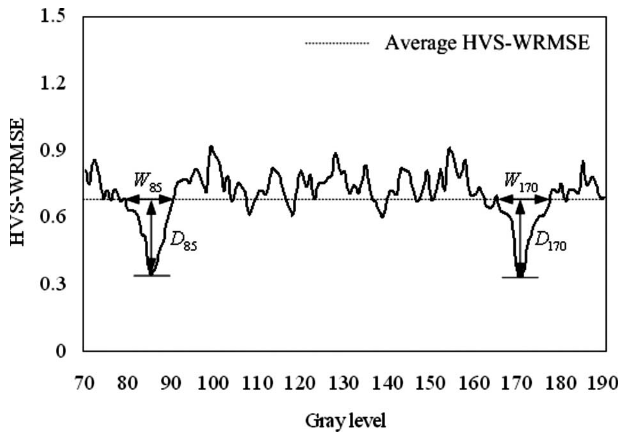

Figure 15. Width and depth of the distinct dipping in the HVS-WRMSE around the printable output tone levels.

Table I. Change in the HVS-WRMSE for varying two control factors around the printable tone levels.

The value of control factors, $(B1_-, B2_-)$	W_{85} (pixels)	D_{85} (HVS-WRMSE)	W_{170} (pixels)	D_{170} (HVS-WRMSE)
When the banding artifact appears	9	0.36	10	0.37
The proposed method with $(B1_-, B2_-)=(84,169)$	7	0.27	8	0.29
The proposed method with $(B1_-, B2_-)=(83,168)$	5	0.18	5	0.17
The proposed method with $(B1_-, B2_-)=(82,167)$	2	0.10	3	0.10
The proposed method with $(B1_-, B2_-)=(81,166)$	1	0.02	0	0.02
The proposed method with $(B1_-, B2_-)=(80,165)$	0	0.04	0	0.08

the distinct dipping in the HVS-WRMSE became smaller due to the reduction in the banding artifacts with the introduction of the dots of the adjacent tone levels. When the control factors approached a certain boundary, the HVS-WRMSE at the intermediate printable tone levels became almost equal to the neighboring values. Beyond this boundary, the HVS-WRMSE began to fluctuate due to the premature introduction of the dots of the adjacent tone levels as mentioned previously.

Similar to these evaluation methods, we determined the most pleasing value of the control factors of dot-dispersion function when the number of printable tone levels was extended to uniform three-tone, five-tone, nine-tone, 17-tone, and 33-tone. It was observed that with decreasing values of the control factor from the intermediate printable tone level of 128, a smoother transition is possible across the band because of the introduction of minority dots. The premature introduction of minority dots in the distribution results in increased graininess. Therefore, with the number of printable tone levels, the value of the control factor that produces a better tone representation and eliminates the undesirable banding artifacts near the printable tone level of 128 is determined as shown in Figure 16. The vertical axis in Fig. 16 stands for the width of the banding region estimated as double the absolute difference between the printable tone level of 128 and the most pleasing value of its corresponding control factor. The width of the banding region slowly decreased with increasing number of printable tone levels and finally converged to five pixels above the 17-tone level. The banding width for both the four-tone and five-tone levels was the same as for the nine pixels.

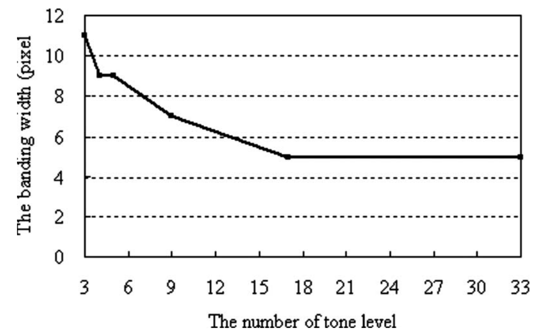

Figure 16. Change in the banding width for the number of printable tone levels.

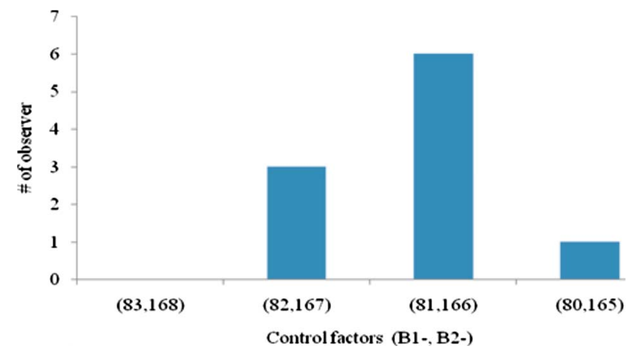

Figure 17. The result of subjective evaluation for four sets of control factors.

EXPERIMENTAL PROCEDURES AND EVALUATIONS

To evaluate the proposed method, an HP Desk-Jet 948C photo printer with four tone levels was used. First, a subjective evaluation of the control factors estimated by HVS-WRMSE was performed using gray ramps multitoned with the proposed method based on four pairs of control factors, $(B1_-, B2_-)=(83,168)$, (82,167), (81,166), and (80,165). Ten observers, seven male, and three female with normal color vision, participated in the experiment. The experiment was performed in a general office environment, and the printed gray ramps examined in close proximity at an arbitrary distance. The observers were asked to select the best multitoned result among the printed gray ramps in terms of the smoothest tone transition around the printable output levels. They used a magnifier for a closer inspection of the distribution of the output pixels. Figure 17 shows the results

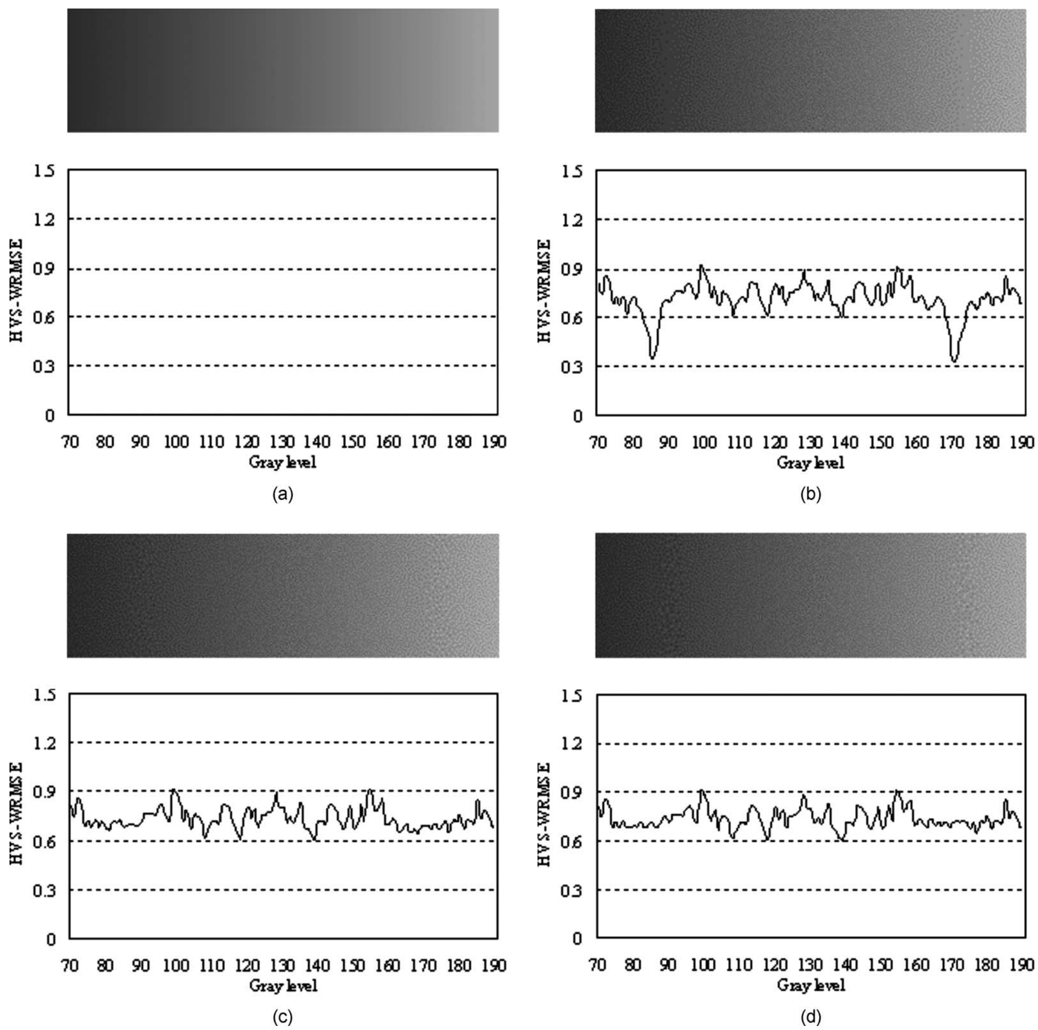

Figure 18. Section of the gray ramps multitoned using three methods and HVS-WRMSE curve when $n=8$ and $m=4$; (a) the original image, (b) the multitoned image using the conventional method with a general threshold scaling function, (c) the multitoned image using the overmodulation technique, and (d) the multitoned image using the proposed algorithm.

of the subjective test, where the horizontal axis shows the four pairs of control factors, and the vertical axis represents the number of observers who chose each specific control factor. From this subjective evaluation, the visually best transition was produced using the proposed method when $B1$ and $B3$ were 81 and 166, respectively. This result was equal to the result obtained using HVS-WRMSE.

To assess the proposed method in comparison with conventional methods, a 256×128 gray ramp image was used. A section (gray level of from 64 to 187) of the original gray ramp image, including the two printable tone levels, 85 and 170, when $n=8$ and $m=4$, is shown in Figure 18(a). The gray ramps multitoned using the three methods are shown in Figs. 18(b)–18(d), respectively. In Fig. 18(c) comparing with Fig. 18(b), dots of adjacent tone levels were introduced by the overmodulation technique to smooth the tone change. However, since most of dots of adjacent tone levels were paired around the printable tone levels, the special correlation and unique characteristics of these patterns had to be added during the screen design in order to achieve a better visual performance. Unlike the examples obtained using other methods, Fig. 18(d) shows a continuous smooth mixture of dots of adjacent tone levels, despite the use of regular screens.

In addition, to compare the banding artifact reduction and the gray-level balance around the intermediate printable tone levels, the HVS-WRMSE, using the HVS model of Sullivan et al.,[7] was computed for each multitoned gray ramps in Figs. 18(b)–18(d). For the conventional method that uses a general threshold scaling function, as shown in Fig. 18(b), there was distinct dipping in the HVS-WRMSE around the intermediate printable tone levels because at the intermediate tone states no multitone error is introduced as the ink for these particular levels is available. Slightly away from these levels, there was a sparse distribution of minority dots over a uniform background. These look like a band, resulting in high visual error in these regions. Thus, to remove the banding artifacts, the HVS-WRMSE distribution had to be equalized. Hence, the optimality criterion is an equalized HVS-WRMSE distribution over the intermediate tone levels. For the overmodulation technique and for the proposed algorithm the HVS-WRMSE value at the interme-

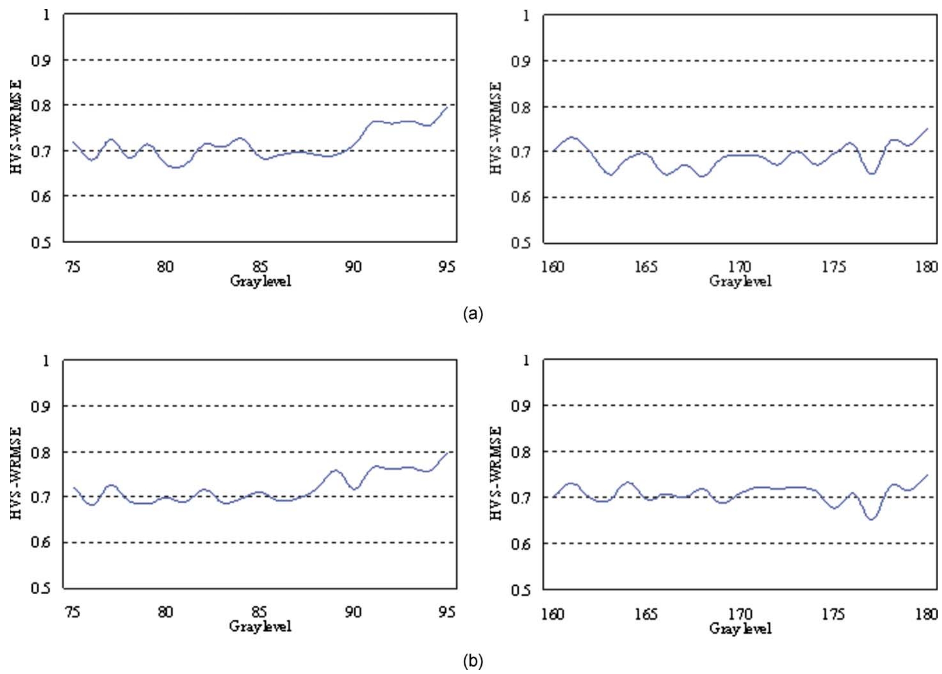

Figure 19. HVS-WRMSE curves around 85 and 170 gray levels; (a) the multitoned image using the overmodulation technique and (b) the multitoned image using the proposed algorithm.

diate printable tone levels had a different distribution, as shown in Figure 19. The HVS-WRMS curve of the propose method in over the intermediate tone levels, 85 and 170, is flatter than that of the method using overmodulation method.

CONCLUSIONS

Conventional multitoning techniques suffer from banding artifacts around the intermediate printable tone levels when a general threshold scaling function is used. These banding artifacts appear to result from a uniform dot distribution near the printable tone levels. Therefore, this article presented a probability model to analyze the banding artifacts, and we investigated the characteristics resulting from and reasons for selection of the number of printable tone levels. After considering the results of this analysis, we proposed HVS-WRMSE, a blue-noise multilevel dithering technique using the interweaving dot-dispersion method to determine the control factors of the dot-dispersion functions. Moreover, when analyzing the increase in the number of printable tone levels, it was evident that the width of the banding region slowly decreased when the number of printable tone levels increased and finally converged to five pixels after 17 tone levels. In experiments, the proposed method produced a moderate reduction in the banding artifacts near the printable tone levels based on an objective evaluation, using the HVS-WRMSE of the multitoned image.

ACKNOWLEDGMENT

This work was supported by the Korea Science and Engineering Foundation (KOSEF) grant funded by the Government of Korea (MEST) (Grant No. 2009-0079859).

REFERENCES

[1] S. Gooran, “A novel hybrid amplitude modulated/frequency modulated halftoning based on multilevel halftoning”, J. Imaging Sci. Technol. **50**, 157–167 (2006).
[2] T. Park, Y. Cho, Y. Kim, C. Lee, and Y. Ha, “Multi-level vector error diffusion for smear artifacts reduction in boundary regions”, J. Imaging Sci. Technol. **48**, 562–572 (2004).
[3] F. Faheem, G. Arce, and D. Lau, “Digital multitoning using gray level separation”, J. Imaging Sci. Technol. **46**, 385–397 (2002).
[4] Q. Yu, K. Parker, K. Spaulding, and R. Miller, “Digital multitoning with overmodulation for smooth texture transition”, J. Electron. Imaging **8**, 311–321 (1999).
[5] Q. Yu, K. Parker, K. Spaulding, and R. Miller, “Improved digital multitoning with over-modulation scheme”, Proc. SPIE **3300**, 362–373 (1998).
[6] T. Park, K. Park, I. Jang, O. Kwon, and Y. Ha, “Banding-artifact reduction using an improved threshold scaling function in multitoning with stochastic screen”, J. Imaging Sci. Technol. **51**, 502–508 (2007).
[7] J. Sullivan, L. Ray, and R. Miller, “Design of minimum visual modulation halftone patterns”, IEEE Trans. Syst. Man Cybern. **21**, 33–38 (1991).
[8] M. Wang, K. Parker, K. Spaulding, Q. Yu, and R. Miller, “Optimal output level selection for multilevel halftoning based on visual experiments using spatially modulated gratings”, J. Imaging Sci. Technol. **47**, 309–326 (2003).
[9] K. Spaulding, R. Miller, and J. Schildkraut, “Methods for generating blue-noise dither matrices for digital halftoning”, J. Electron. Imaging **6**, 208–230 (1997).
[10] Y. Kim, Y. Cho, C. Lee, and Y. Ha, “Halftoning method using dispersed CMY dithering and blue noise mask”, J. Imaging Sci. Technol. **48**, 37–44 (2004).
[11] T. Mitsa and K. Parker, “Digital halftoning technique using a blue-noise mask”, J. Opt. Soc. Am. A **9**, 1920–1929 (1992).
[12] M. Wang and K. Parker, “Properties of jointly-blue noise masks and applications to color halftoning”, J. Imaging Sci. Technol. **44**, 360–370 (2000).
[13] Y. Kwon, Y. Kim, C. Lee, and Y. Ha, “Modified jointly blue noise mask approach using S-CIELAB color difference”, J. Imaging Sci. Technol. **46**, 543–549 (2002).
[14] R. Ulichney, “Dithering with blue noise”, Proc. IEEE **76**, 56–79 (1988).
[15] N. Damera-Venkata and B. Evans, “FM halftoning via block error diffusion”, *Proc. IEEE International Conference on Image Processing* (IEEE, Piscataway, NJ, 2001), Vol. **2**, pp. 1081–1084.